

A CRYOGENIC CURRENT COMPARATOR FOR THE LOW-ENERGY ANTIPROTON FACILITIES AT CERN

M. Fernandes*, The University of Liverpool, U.K. & CERN, Geneva, Switzerland

J. Tan, CERN, Geneva, Switzerland

C. Welsch, Cockcroft Institute & The University of Liverpool, U.K

R. Geithner, R. Neubert, T. Stöhlker, Friedrich-Schiller-Universität &

Helmholtz Institute Jena, Jena, Germany

M. Schwickert, GSI, Darmstadt, Germany

Abstract

Several laboratories have shown the potential of Cryogenic Current Comparators (CCC) for an absolute measurement of beam intensity down to the nA level. This type of current monitor relies on the use of Superconducting QUantum Interference Device (SQUID) magnetometers and superconductor magnetic shields. CERN, in collaboration with GSI Helmholtz Centre for Heavy Ion Research, Jena University, and the Helmholtz Institute Jena are currently developing an improved version of such a current monitor for the Antiproton Decelerator (AD) and Extra Low ENergy Antiproton (ELENA) rings. The primary goals are a better current measurement accuracy and overall enhanced system availability. This contribution presents the design of the CCC, an estimation of its resolution, dynamic limitations of the SQUID, as well as a description of the modifications to the coupling circuit and cryostat that were required to optimize the monitor for the anticipated beam parameters. First results from beam measurements are also presented. To our knowledge these are the first CCC beam current measurements performed in a synchrotron and the first to be performed with both coasting and bunched beams.

LOW-INTENSITY BEAMS CURRENT MEASUREMENT

Low-intensity charged particle beams present a considerable challenge for existing beam current diagnostics [1]. This is particularly significant for coasting beams with average currents below 1 μA which is the minimum resolution of standard DC Current Transformers. Other monitors, such as AC Current Transformers or Schottky monitors (currently in use in AD) are able to measure low-intensity beam currents, but neither can simultaneously provide an absolute measurement, with a high current and time resolution, which is at the same time independent of the beam profile, trajectory and energy.

At CERN's low-energy antiproton decelerators, the AD and the ELENA (currently under construction) rings, circulate both bunched and coasting beams of antiprotons with average currents ranging from 300 nA to 12 μA . Having a

current measurement with the above mentioned characteristics would benefit the machine operation and optimization.

To meet these requirements, a low-temperature SQUID-based Cryogenic Current Comparator (CCC) is currently under development [2, 3]. Similar devices have already been developed for electrical metrology [4, 5], and have already been used for beam current measurements in particle accelerator [6, 7]. The current project, is a collaboration between CERN, GSI, Jena University and Helmholtz Institute Jena to develop this technique further.

The main design specifications for the monitor are: beam current resolution < 10 nA; and measurement bandwidth of 1 kHz.

Overview of the Functioning Principle of the CCC

The CCC (see schematic in Fig. 1) works by measuring the magnetic field induced by the particle beam current. This field is concentrated in a high-permeability ferromagnetic pickup core, from which it is coupled into the SQUID sensor. These are highly sensitive magnetic flux sensors that permit sensing the weak fields created by the beam. A superconducting magnetic shield structure around the pickup core, as described in [7, 8], renders the coupled magnetic field nearly independent of the beam position and makes the system practically immune to external magnetic field perturbations. The unique advantages of the CCC monitor

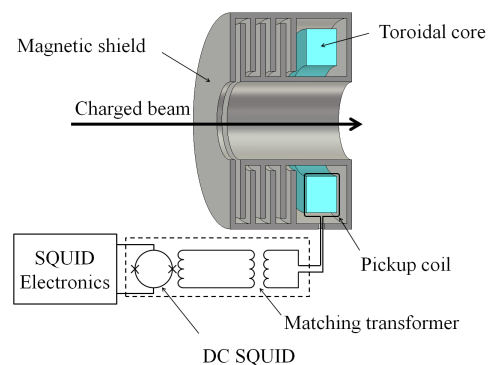


Figure 1: Schematic of the CCC.

are its ability to measure the average current of both coasting and bunched beams with nA resolution, as has been demonstrated by other laboratories. Previous installations of the CCC for beam current measurements were, however, usually

* Funded by the European Union's Seventh Framework Programme for research, technological development and demonstration under grant agreement no 289485.

restricted to slowly extracted beams in transfer lines. When used for the high-resolution measurement of bunched beams on a circular machine, the stability limitation of SQUIDS, when using a Flux-Locked Loop (FLL) read-out scheme [9], and the immunity to mechanical and electromagnetic (EM) perturbations soon become limiting factors.

CCC CHARACTERISTICS

The superconducting shield and pickup core of the AD CCC were developed by GSI, Jena University and Helmholtz Institute Jena. This core has a single turn inductance $L_P = 104 \mu\text{H}$, while the SQUID device has an input coil self-inductance $L_i = 1 \mu\text{H}$ and a mutual inductance $M_i = 3.3 \phi_0/\mu\text{A}$ ¹.

Coupling Circuit and Resolution

The circuit shown in Fig. 2 couples the beam current signal into the SQUID. An appropriate choice of the pickup core and matching transformer are important to optimize the strength of the coupled signal, and thus improve the Signal to Noise Ratio (SNR). The theoretical dc-gain of this circuit (flux coupled to the SQUID per unit of beam current) is $S_{IB} = \Phi_S(t)/I_B(t) = 10.5 \phi_0/\mu\text{A}$ [3] (in SQUID systems literature it is more commonly quoted the inverse quantity $95.2 \text{ nA}/\phi_0$). The measured gain of the coupling circuit,

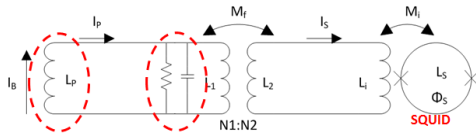


Figure 2: Coupling circuit that converts the beam current into a magnetic flux to be measured by the SQUID.

obtained after factoring the gain of SQUID/FLL electronics, was:

- Calibration winding: $S_{IB} = 10.46 \phi_0/\mu\text{A}$,
- Beam current wire: $S_{IB} = 10.44 \phi_0/\mu\text{A}$.

Which are both very close to the computed theoretical value.

Low-pass Filtering in the Coupling Circuit

Flux-Locked Loop (FLL) SQUID systems impose a maximum limit on the slew-rate of the signal to be measured [10]. In order for the SQUID to keep a constant working point an equilibrium between FLL bandwidth, system noise and maximum slew-rate needs to be observed [3]. In modern SQUID/FLL systems, such as the one used in the current AD CCC, the maximum slew-rate of the magnetic flux coupled to the SQUID needs to be $< 5 M\phi_0/\text{s}$

The nominal beam injected in the AD has the following parameters: $f_{\text{rev}} = 1.59 \text{ MHz}$, $h = 6$ with 4 buckets filled, $4\sigma_t^{\text{bunch}} = 30 \text{ ns}$ and $Q^{\text{bunch}} = 1.25 \times 10^7 e$. When such a

¹ $\phi_0 = 2.0678 \times 10^{-15} \text{ Wb}$ is the magnetic flux quantum which is the unit commonly used for magnetic flux when dealing with SQUID systems.

beam is injected the average current jumps from 0 to $12 \mu\text{A}$, and the slew-rate of the flux coupled to the SQUID reaches $400 M\phi_0/\text{s}$ (assuming a constant gain of the coupling circuit). To reduce the magnetic flux slew-rate, without decreasing the low-frequency coupling strength, a low-pass filtering has been implemented. In order to filter the input signal

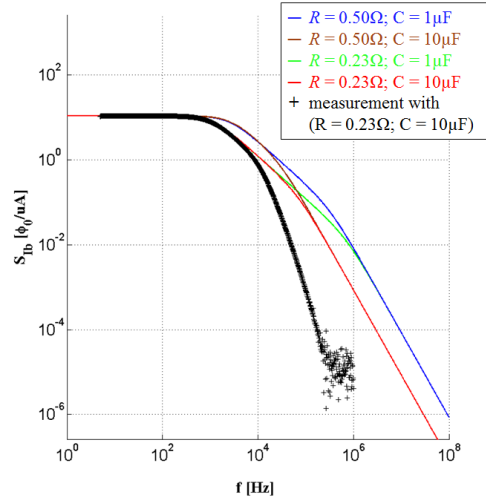


Figure 3: Theoretical frequency response of the coupling circuit alone, for various values of R and C. And laboratory measurement of the frequency response of the complete system (coupling circuit plus cryostat) using a beam simulating wire passing through the cryostat beam pipe (in black).

an RC-parallel filter was added to the primary side of the coupling circuit of the CCC. The theoretical frequency response for different values of the RC values are shown in Fig. 3. The measured transfer function closely follows the theoretical curve until one decade after the cut-off frequency. For higher frequencies a stronger attenuation is observed due to the fact that this measurement takes into account the complete system, coupling circuit plus cryostat (described in next section). Laboratory measurements of different configurations for the coupling circuit filter were also presented by R. Geithner during IBIC'15 conference.

This filter, however, only reduces the maximum slew-rate of the signal coupled to the SQUID, during AD antiproton beam injection to $37 M\phi_0/\text{s}$. This is still one order of magnitude above the stability limit of the SQUID/FLL system.

Low-pass Filtering in the Cryostat

In order to further reduce the slew-rate of the signal coupled to the SQUID it was decided to add an RF-bypass to the ceramic gap in the beam pipe. This capacitance in parallel with the high-resistance metallisation on the surface of the ceramic forces the high frequency components of the beam induced mirror current to flow through the beam pipe instead of the outer shell of the cryostat. Thus removing the high-frequency components of the magnetic field reaching the CCC toroid and in so-doing providing the desired low-pass filtering effect. In order to dimension the RF-bypass

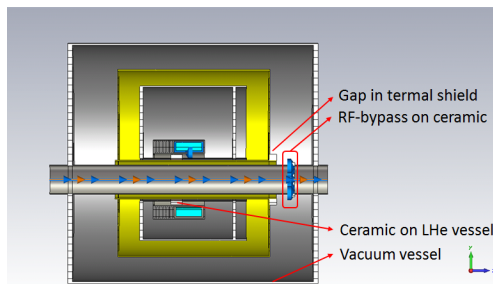


Figure 4: Simplified model of the real cryostat used in time-domain simulation of a single bunch. The CCC shield is shown, but was not considered for the simulation.

the following procedure was followed. First a simulation for a single AD bunch at injection was performed using the Wakefield Solver of the CST Studio Suite. In this simulation a simplified model of the fabricated cryostat was used (see Fig. 4). Since this was a relatively low frequency problem, the RF-bypass impedance was modelled by lumped elements. The signal coupled to the pickup was obtained via a magnetic field probe. By scanning several values of the total capacitance across the ceramic gap, the bunch responses in Fig. 5 were obtained.

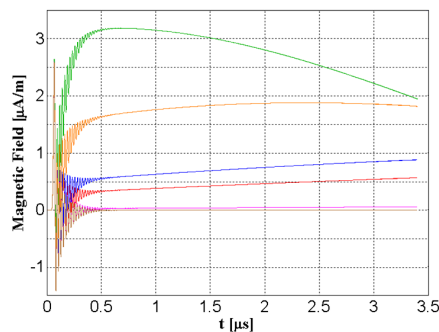


Figure 5: Time domain simulation of the magnetic field coupled to pickup core, induced by the passage of a single bunch of the AD injection beam.

Each iteration of this simulation took a considerable amount of time, so it was not possible to run it for a period of time long enough for the magnetic field signal to decay to zero. Hence the remaining part of signal had to be extrapolated, and this was done using a polynomial function. Despite its limitations in estimating the signal evolution, this analysis should, in principle, always result in an overestimation of the magnetic flux slew-rate of the bunch train, which is the quantity we want to limit.

Having an estimation of the magnetic signal induced by the passage of a single bunch, the signal induced by the passage of the bunch train was synthesised assuming linearity of the system.

In order to use this signal as an input to the transfer function of the coupling circuit in Fig. 2, and estimate the combined filtering effects, the magnetic signal of the bunch train

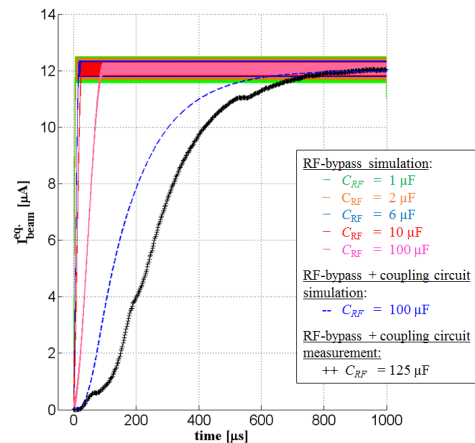


Figure 6: Simulation of the signal (referred to equivalent beam current) coupled to the SQUID at AD beam injection, considering the RF-bypass alone and also the combined effect with the coupling circuit filter. And laboratory measurement using a signal generator passing a similar current signal through a beam simulating wire.

was normalized to an equivalent beam current. For this, the steady-state beam average current $I_{\text{beam}}^{\text{avg}} = 12 \mu\text{A}$ was used as a normalization factor. The equivalent beam current signals for the different values of capacitance in the RF-bypass are shown in Fig. 6.

Simulating the passage of these equivalent current signals through the low-pass filtered coupling circuit, one obtains the values in Table 1 for the maximum slew-rate that the SQUID will be subjected to during AD beam injection:

Table 1: Maximum Estimated SQUID Flux Slew-rate for Diffent RF-bypass Capacitance Values

RF-bypass C [μF]	1	2	6	10	100
Max. slew-rate [$M\phi_0/s$]	6.06	6.01	5.84	5.63	2.83

For $C \geq 100 \mu\text{F}$ the maximum slew-rate falls below the stability limit of $5 M\phi_0/s$. The value used in the RF-bypass capacitance in the AD implementation of the monitor is therefore $C = 125 \mu\text{F}$. In Fig. 6 is shown the measured response of the complete system to a current identical to AD injection passing trough a beam simulating wire.

AD BEAM MEASUREMENTS

The newly fabricated cryostat and CCC were installed in the AD-ring before AD operation started in 2015, and beam measurements have been taken on various occasions. Since the CCC measures primarily the beam current, while the most relevant figure of merit of the AD ring operation is the “intensity” or number of accumulated particles, the current

measurement needs to be normalized against the particles velocity.

Current Measurement

During commissioning and before the first beams were injected two issues were identified that have an impact on the performance of the current measurement. Excessive perturbations were observed at frequencies that are odd multiples of 50 Hz and pulsing the bunch rotation cavities (occurring once per cycle, around 50 μ s after injection) was seen to cause a significant flux jump in the SQUID/FLL working point. Both these limitations can be seen in the middle plot

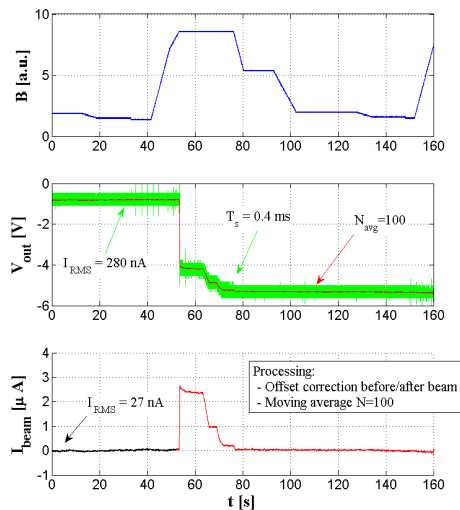


Figure 7: Top Plot: Magnetic Cycle of AD Dipoles in arbitrary Units. Middle plot: SQUID/FLL raw signal of beam current (in green), and same signal filtered with a moving average (in red). Bottom plot: calibrated beam current measurement after filtering and baseline recovery (before beam injection and after extraction).

of Fig. 7, with the green trace showing the raw SQUID/FLL voltage signal. The RMS noise (caused essentially by the 50 Hz harmonics) amounts to 275 nA of beam current, while the flux jump is also quite clear as the measured current decreases when it should increase on beam injection.

Both these limitations can be mitigated by post-processing the acquired raw signal. As a first approach the excessive perturbation was filtered out using a time-domain moving average low-pass filter. The flux jump at injection can be corrected by adjusting the offset of the signal before and after injection, knowing that before injection and after extraction the beam current has to be zero.

In Fig. 7 is shown a beam commissioning cycle where the beam was entirely lost during the first cooling plateau. The instant where beam is lost are clearly visible, this represents a clear improvement over the Schottky measurement used to date. This demonstrated that the CCC can be an invaluable tool both for reducing the time needed to setup the beam and for increasing machine efficiency.

ISBN 978-3-95450-176-2

Intensity Measurement

The number of circulating antiprotons can be obtained by normalizing the current measurement with the particle velocity (in the AD, $\beta_{inj.} = 0.97$ and $\beta_{ej.} = 0.11$). The velocity profile was calculated from the magnetic cycle of the dipole magnets.

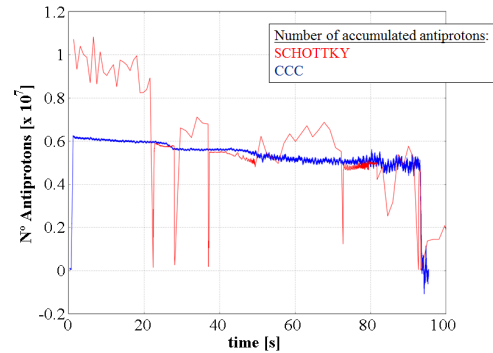


Figure 8: Comparison of the “intensity” (number of antiprotons) measurement between the longitudinal-Schottky and the CCC monitors, during one AD cycle (with 10% of nominal intensity).

From Fig. 8 it is possible to observe that the CCC measurement is much more precise during the coasting beam phases than the Schottky one. One limitation, inherent to the normalization method, is that for small β the errors in the current measurement due to the 50 Hz harmonics are greatly amplified.

CONCLUSION

The different aspects of a CCC current monitor adapted to the measurement of the low-intensity antiproton beams in AD have been presented. A monitor based on this design has been installed, and first beam measurements have been reported. To our knowledge these are the first CCC beam current measurements performed in a synchrotron, on both coasting and bunched beams.

The two major challenges in the adaptation of this type of monitor to the dynamic range and bunched beam of the AD were to guarantee the SQUID/FLL stability when faced with a large input slew-rate at injection, and to avoid the excess noise contamination which may limit the superior current resolution that CCC monitors have shown in other laboratories.

While the first has been successfully addressed the second is still under investigation. It is suspected that this noise may be due to currents flowing in the beam pipe that are then picked up by the monitor. The RF-bypass (needed in order to reduce the beam signal slew-rate) installed in the ceramic gap may therefore be responsible for these two limitations. One solution could be to move this to the gap in the thermal shield. Such optimization is still underway in order to deliver the CCC as a fully operational beam current measurement device for the AD.

ACKNOWLEDGMENT

The authors would like to acknowledge the work and support of Andrew Lees, Torsten Koettig and Conor Sheehan from CERN's TE-CRG group, who are providing the cryogenic system design, including the cryostat mechanical design, Jean-Pierre Brachet and Didier Lombard from CERN's EN-MME group, and respective teams responsible for the cryostat fabrication, and Ewa Oponowicz and Michael Ludwig from CERN's BE-BI group, who developed the acquisition software. I also thank Patrick Odier, Jeroen Bellemann from CERN, Febin Kurian, Marcus Schwickert and Thomas Sieber from GSI, René Geithner from Helmholtz Institute Jena and Ralf Neubert from Jena University for the many fruitful discussions. Finally I acknowledge the oPAC network support which has made this work possible.

REFERENCES

- [1] D. Belohrad, "Beam Charge Measurements," WEOC01, DIPAC2011 proceedings.
- [2] M. Fernandes et al., "Cryogenic Current Comparator for Low Intensity Beam Current Measurement", MOPF25, IBIC'13 Proceedings, Oxford, U.K. (2013)
- [3] M. Fernandes et al., "A Cryogenic Current Comparator for the Low Energy Antiproton Facilities at CERN", WEPF04, IBIC'14 Proceedings, Monterey, U.S.A (2014)
- [4] I.K. Harvey, Rev. Sci. Instrum. 43 (1972) 1626.
- [5] W. Vodel et al., "Chapter 9.6: SQUID-Based Cryogenic Current Comparators", In: P. Siedel, Applied Superconductivity Handbook on Devices and Applications, Volume2, (Weinheim: Wiley-VCH, 2015).
- [6] R. Geithner et al., "A SQUID-based Beam Current Monitor for FAIR/CRYRING", WECZB1, IBIC'14 Proceedings, Monterey, U.S.A. (2014)
- [7] A. Peters et al., "A cryogenic current comparator for the absolute measurement of nA beams," BIW98, Stanford, May 1998, (p. 163), AIP conference proceedings.
- [8] K. Grohmann et al., Cryogenics 16(10) (1976) 601.
- [9] D. Drung and M. Muck, "Chapter 4: SQUID Electronics", In: J. Clarke and A. Braginski, The SQUID Handbook. Vol. I: Fundamentals and Technology of SQUIDS and SQUID Systems. Materials and Manufacturing Processes, (Weinheim: Wiley-VCH, 2005).
- [10] R. H. Koch, "Maximum theoretical bandwidth and slewrates of a dc SQUID feedback system," IEEE Transactions on Applied Superconductivity 7(2), p. 3259 (1997).